

Enhancement of second harmonic generation signal in thermally poled glass ceramic with NaNbO_3 nanocrystals

Artem Malakho, Evelyne Fargin,^{a)} and Michel Lahaye

Institut de Chimie de la Matière Condensée de Bordeaux—UPR 9048 CNRS, Chateau Brivazac, Avenue du Dr. Schweitzer, 33608 Pessac Cedex, France

Bogdan Lazoryak and Vladimir Morozov

Department of Chemistry, Moscow State University, Moscow 119899, Russia

Gustaaf Van Tendeloo

EMAT, University of Antwerp, Groenenborgerlaan 171, B-2020 Antwerp, Belgium

Vincent Rodriguez and Frederic Adamietz

Laboratoire de Physico-Chimie Moléculaire, UMR 5803 CNRS, Université Bordeaux I, 351 cours de la Libération, 33405 Talence Cedex, France

(Received 1 January 2006; accepted 27 May 2006; published online 22 September 2006)

Glass ceramic composites were prepared by bulk crystallization of NaNbO_3 in sodium niobium borate glasses. A homogeneous bulk crystallization of the NaNbO_3 phase takes place during heat treatments that produces visible-near infrared transparent materials with ~ 30 nm NaNbO_3 nanocrystallites. Upon thermal poling, a strong Na^+ depleted nonlinear optical thin layer is observed at the anode side that should induce a large internal static electric field. In addition, the $\chi^{(2)}$ response of the poled glass ceramic composites increases from 0.2 up to 1.9 pm/V with the rate of crystallization. Two mechanisms may be considered: a pure structural $\chi^{(2)}$ process connected with the occurrence of a spontaneous ferroelectric polarization or an increase of the $\chi^{(3)}$ response of the nanocrystallites that enhances the electric field induced second harmonic generation process.

© 2006 American Institute of Physics. [DOI: 10.1063/1.2259816]

I. INTRODUCTION

Glass does not exhibit second order optical nonlinearity due to its inversion symmetry. Nevertheless, some techniques were developed to induce quadratic nonlinear optical (QNLO) responses in glass-based materials. One of them—thermal poling—was reported silica glasses by Myers *et al.*¹ This technique consists in applying a direct-current (dc) electric field to the glass at an elevated temperature and then cooling the temperature before removing the electric field. As a result, a nonlinear layer with a thickness of 1–10 μm is created at the anode surface of the glass due to a charge migration. A model of built-in internal electric field created in thin anode layer is proposed to explain the origin of QNLO in thermally poled glasses.² The effect of this electric field combined together with the third order nonlinearity of the glass, $\chi^{(3)}$, determines the amount of second order optical susceptibility, $\chi^{(2)}$.³

$$\chi^{(2)} = 3\chi^{(3)}E_{\text{dc}}. \quad (1)$$

Recent advances in studies of thermal poling have resulted in commercial electro-optical switches and frequency converters based on poled silica glass fibers.⁴ However, the optical nonlinearity is rather weak in silica glasses (~ 0.1 pm/V) whereas relative large values of $\chi^{(2)}$ were induced in thermally poled niobium borophosphate (~ 5 pm/V) (Ref. 5) and chalcogenide glasses

(~ 8 – 10 pm/V).⁶ Yet, the maximal values of $\chi^{(2)}$ gained in thermally poled glasses are still one order of magnitude below $\chi^{(2)}$ responses of the best ferroelectric crystals (LiNbO_3 — $\chi^{(2)} \sim 70$ pm/V).⁷

Concurrently, promising results have been achieved in the preparation of glass ceramic composites containing crystallites of ferroelectric phases.⁸ Composite materials prepared by surface or bulk crystallization may show a second order nonlinear optical efficiency comparable to that of ferroelectric crystals.⁹ However, the particle size should be much less than the wavelength of light to provide good transparency and optical homogeneity of the composites. At the same time, the ferroelectric properties and the optical nonlinearity of the composites decrease with the crystal size. Numerous investigations provide examples of compromises between optical transparency and ferroelectric and QNLO properties of glass ceramic composites with domains of particle size ranging between 20 and 200 nm.^{8,10,11}

Some recent studies have shown that thermal poling may improve the optical nonlinearity of glass ceramics containing ferroelectric crystals.^{12,13} For example, Tamagawa *et al.* have reported an enhancement of the second harmonic generation (SHG) signal in a crystallized glass with composition of $15\text{K}_2\text{O}-15\text{Nb}_2\text{O}_5-68\text{TeO}_2-2\text{MoO}_3$ containing ferroelectric crystals with ~ 20 nm size.¹² The SHG signal, after thermal poling, was measured to be 6–20 times higher than in the unpoled glass ceramic. An increase of the spontaneous polarization in ferroelectric nanocrystals was assumed to be the

^{a)}Author to whom correspondence should be addressed; electronic mail: fargin@icmcb-bordeaux.cnrs.fr

main result of the thermal poling that usually induces electric field induced second harmonic generation (EFISHG) responses in poled glasses.

This article reports the experimental observation of $\chi^{(2)}$ enhancement in thermally poled sodium niobium borate glasses with nanocrystallization of NaNbO_3 . The second order nonlinear optical susceptibility of thermally poled crystallized glass ceramics was found to be ten times larger than in poled noncrystallized glasses. The effect of crystallization on both transparency and nonlinear optical properties of the glasses is discussed.

II. EXPERIMENT

Glasses with nominal composition of $0.7\text{Na}_2\text{B}_4\text{O}_7 + 0.3\text{Nb}_2\text{O}_5$ (called hereafter NBN30) were prepared using a conventional melt-quenching method. Commercial reagent-grade powders $\text{Na}_2\text{B}_4\text{O}_7$ (Alfa Aesar, 99.5%) and Nb_2O_5 (Cerac, 99.99%) were mixed and melted in a platinum crucible at 1050°C for 40 min. The melt was poured onto a brass plate and quenched by sandwiching with another brass plate. Quenched glass was annealed at 300°C for 24 h. The glass transition, T_g , and crystallization, T_x , temperatures were determined using differential thermal analyses (DTA) at a heating rate of $10^\circ\text{C}/\text{min}$.

As-prepared and heat-treated samples were examined by x-ray diffraction (XRD) analysis at room temperature using $\text{CuK}\alpha$ radiation (Philips Xpert, graphite monochromator). For transmission electron microscopy (TEM) crushed samples were deposited on holey carbon grids. TEM observations and electron diffraction (ED) together with energy dispersive x-ray (EDX) analysis were made on a Philips CM20 microscope, operating at 200 kV. EDX analysis was performed on the CAMECA SX100 spectrometer. Concentrations of the Na and Nb were measured on cross sections of the poled samples. Relative accuracy of atomic concentration values for Na and Nb is $\sim 5\%$.

As-prepared glasses and glass ceramic composites were cut and polished on both sides to gain optical quality. Absorption spectra were recorded in the wavelength range of 200–2500 nm at room temperature using a Cary 5000 ultraviolet-visible-near infrared (UV-vis-NIR) spectrophotometer. Thermal poling of glasses and glass ceramic composites was performed at 180°C . Samples were sandwiched between a silicon wafer at the anode and a thin borosilicate glass plate at the cathode. The poling voltage, 3 kV, was applied for 30 min. Then, the samples were cooled down before the external voltage was removed.

Measurements of SHG responses of as-prepared and crystallized glasses were performed before and after thermal poling. The experimental setup used for QNLO measurements has been described earlier.¹⁴ The source was a Q-switched Nd:YAG (yttrium aluminium garnet) laser operating at a wavelength of 1064 nm. The polarized source beam was split into two branches by a beam splitter. One branch recorded the fundamental intensity with a Ge photodiode, and the other, which passed through a polarizer to adjust its polarization, was focused on the sample with a spot of $100\ \mu\text{m}$ diameter. The 2ω transmitted signal was detected

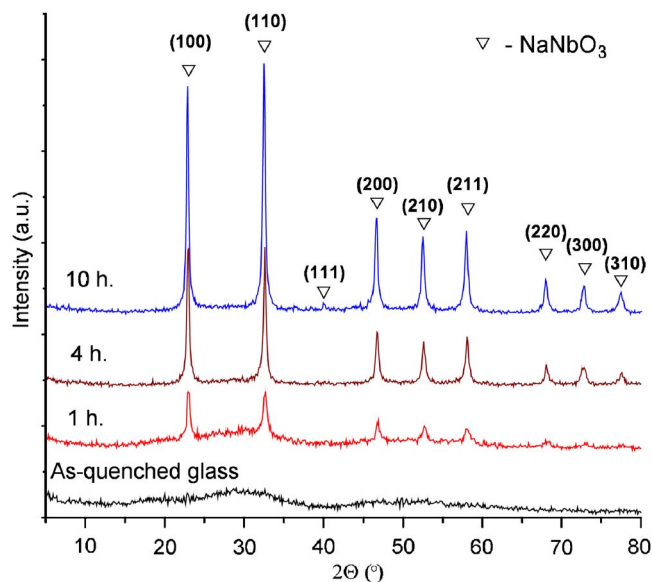


FIG. 1. (Color online) XRD patterns of as-quenched NBN30 glass and crystallized samples obtained by heating at the 530°C during 1, 4, and 10 h. Indicated Miller indices correspond to cubic NaNbO_3 phase (space group $Pm\bar{3}m$ (Ref. 23]).

by a first photomultiplier and averaged over 50 pulses. The calibration of the SHG intensities is obtained using a quartz z -cut plate, taking $\chi_{xxx}^{(2)} = 0.6\ \text{pm}/\text{V}$ at 1064 nm as reference.⁷ Linear refractive indices were estimated at ω and 2ω with a second photomultiplier by collecting the corresponding 2θ reflected wave around the Brewster angle over the 10° – 80° θ range. The SHG Maker fringes were analyzed using a general ellipsometric analysis for planar multilayered media.¹⁴ The Maker fringe signals [in pp and sp polarization configurations, where pp (sp) means p -polarized (s -polarized) incident pump beam and p -polarized transmitted second harmonic beam] were recorded for the studied samples.

III. RESULTS AND DISCUSSION

Values of glass transition, T_g , and crystallization, T_x , temperatures for NBN30 glass are 441 and 530°C , respectively. A two-step heat treatment was performed to obtain crystallized glasses. First, NBN30 glass samples were annealed at 420°C for 24 h for nucleation and afterwards samples were crystallized at 530°C for 1, 4, and 10 h. A homogeneous bulk crystallization of the NaNbO_3 phase takes place during the heat treatments. All diffraction lines on the XRD patterns of crystallized glasses correspond to the cubic NaNbO_3 phase (Fig. 1). The lattice parameter a of the crystallized phase was determined by the least-squares technique. The determined value of $a \sim 3.89$ – 3.90 for the crystallized samples is close to that of pure crystalline cubic NaNbO_3 [space group $Pm\bar{3}m$ (Ref. 23)]. The overall intensities of the diffraction lines increase whereas their widths slightly decrease upon increasing the time of heating. An estimation of the average crystal size from full width at half maximum (FWHM) of the diffraction lines was made using Scherrer's formula and resulted values are $\sim 30(10)$ nm. The

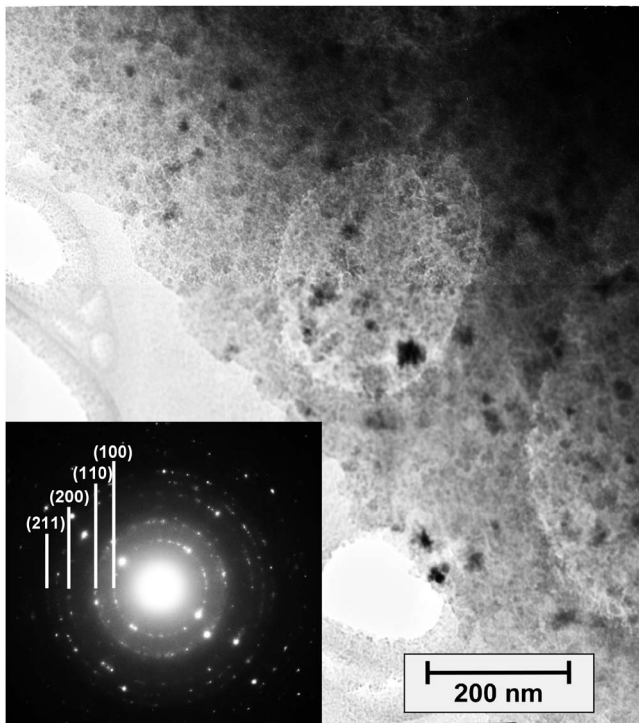


FIG. 2. Transmission electron images of a crystallized NBN30 glass (530 °C, 1 h). The inset shows the corresponding SAED pattern. Only the most intense rings are indexed.

absence of surface crystallization and bulk crystallization of large ($>1 \mu\text{m}$) particles was checked by optical microscopy.

TEM observations show that NBN30 glass samples crystallized at 530 °C for 1 h consist of nanosized particles with an irregular shape and various dimensions, ranging from 10 to 40 nm (Fig. 2). The large area of circular shape with size of about 200 nm corresponds to holey carbon grid deposited as a conductive substrate for analyzed samples. The size of the particles is in good agreement with the values calculated from XRD data (~ 30 nm). The inset shows the electron diffraction pattern corresponding to a selected area. The ring pattern could be indexed as the cubic NaNbO_3 structure: in Fig. 2, for clarity, only the most intense rings are indexed. The d spacings of the ring pattern are similar to that of the XRD patterns of crystallized glass containing the NaNbO_3 phase (Fig. 1).

The transmission spectra of as-quenched and crystallized glasses are reported in Fig. 3. A scattering of light merges from the UV front absorption edge in all crystallized samples, in connection with the increasing size of the crystal nanoparticles. The sample heated at 530 °C for 1 h has a good transparency in the visible wavelength range, while glasses crystallized during 4 and 10 h are opalescent; meanwhile all crystallized glasses are transparent in the near infrared range (>900 nm). Thus, the size of the particles in this transparent glass ceramic should be at least 30 times less than the wavelength of light. Such a strong scattering of light on small particles is observed because of the huge difference of the refractive indices of NBN30 glass matrix ($n_{532} = 1.70$) and of the crystallized NaNbO_3 particles ($n_{532} \sim 2.20$).

As-prepared and crystallized glasses give no SHG sig-

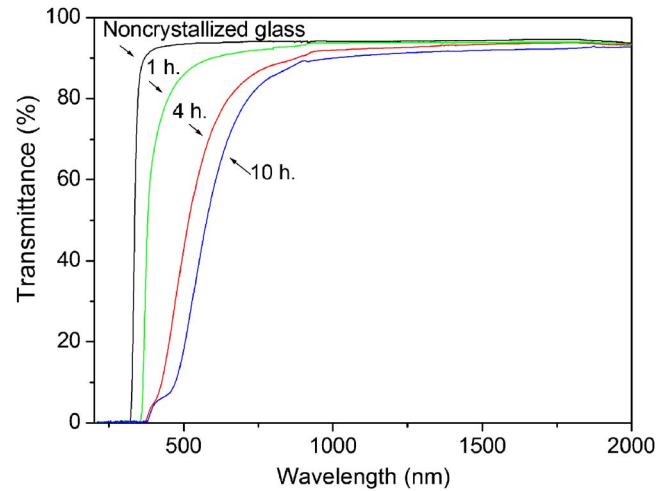


FIG. 3. (Color online) Optical transmission spectra (uncorrected for reflection) for as-prepared NBN30 glass and crystallized samples obtained by heating at 530 °C during 1, 4, and 10 h.

nal. To induce a second order optical nonlinearity, all samples have been thermally poled in the same conditions: $T=180$ °C, $U=3$ kV, and time=30 min. After the thermal poling treatment, a SHG signal could be detected in all samples. The shapes of the Maker fringe patterns obtained in transmission indicate that a second order nonlinearity is induced in a thin layer at the anode side of the poled samples. A net polishing of the anode surface erases the SHG response.

To collect the Maker fringe patterns in transmission, the anodic NLO layer of each sample was oriented toward the detection unit, so the laser beam enters first the cathode side of the sample and goes out through the anode side. As mentioned above, the glass ceramic composites scatter slightly light at 1064 nm and, as a result, we have limited in this way the SHG scattering losses. For the analyses of the Maker fringes, we used a two layer model: one isotropic layer with thickness equal to the total thickness of the plate and one NLO layer of thickness of a few micrometers. Two components of the nonlinear susceptibility tensor χ_{zzz} and χ_{zxx} were adjusted in accordance with the polar symmetry generated by the poling treatment ($C_{\infty v}$ in the Schoenflies notation). Additionally, following the EFISHG model,⁵ we have admitted the relation $\chi_{zzz}=3\chi_{zxx}$. The SHG Maker fringe patterns could be nicely fitted as illustrated in Fig. 4. The fitted values of the second order optical susceptibilities $\chi^{(2)}$, refractive indices, and estimated thicknesses for all nonlinear layers are gathered in Table I. The longitudinal second order optical susceptibility χ_{zzz} is rather weak in poled noncrystallized glass ($\chi^{(2)} \sim 0.2$ pm/V) but it increases progressively with the rate of crystallization of the NaNbO_3 phase. The values of $\chi^{(2)}$ for samples annealed at 530 °C from 1 to 10 h increase by a factor of ~ 4 .

The migration of sodium in the thermally poled samples was studied by EDX analysis. A thermally poled noncrystallized glass and a glass heated at 530 °C for 4 h were cut and their cross sections along the poled layer thickness have been analyzed. Only the Na and Nb concentrations could be measured with the Na $K\alpha$ and Nb $L\alpha$ fluorescent lines. Oxygen

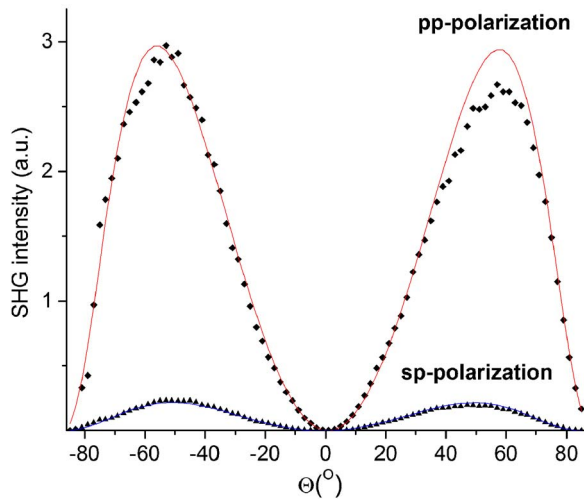


FIG. 4. (Color online) Experimental (points) and calculated (solid lines) SHG Maker fringe patterns (transmission) of an NBN30 glass crystallized at 530 °C during 4 h.

and boron concentrations were not quantified. The concentration of niobium was assumed to be constant in the poled glasses and it was taken as a reference to quantify the sodium migration. The Na/Nb atomic ratios along the anode cross section of a noncrystallized and a crystallized poled glass are both reported in Fig. 5. A layer with a lower concentration of sodium is evidenced at the anode surface of the noncrystallized poled glasses (Fig. 5). A similar migration has been reported earlier in thermally poled borophosphate glasses with sodium and niobium and the depleted layer was found to have the same thickness as the NLO layer.⁵ However, unlike poled borophosphate glasses, the profile of the sodium depletion in the as-prepared NBN30 glass is rather smooth and the concentration of sodium never decreases to zero in the depleted layer. In the crystallized sample, a migration of sodium is also observed but it is less pronounced than in pure NBN30 glass. The Na/Nb ratio at the anode surface of the poled crystallized glass is close to 1 and it linearly increases along the cross section on $\sim 4 \mu\text{m}$. The concentration of sodium in the NLO layer is noticeably higher than in poled noncrystallized glasses. The mobility of the sodium ions located among the crystallized particles should be lower, and probably only sodium ions involved in the glass matrix of composite do migrate under the poling electric field. This minimal Na/Nb ratio ≈ 1 may be explained assuming that most of the niobium is located in the crystallized NaNbO_3

TABLE I. Refractive indices and optical parameters obtained from the Maker fringe analyses for as-prepared NBN30 glass and glass ceramic samples.

Sample	Refractive indices n (± 0.02)		$\chi_{zzz}^{(2)}$ (pm/V) ($\pm 10\%$)	Layer thickness (μm) (± 0.1)
	1064 nm	532 nm		
Pure NBN30 glass	1.64	1.70	0.2	2.7
NBN30, 530 °C, 1 h	1.64	1.72	0.5	2.5
NBN30, 530 °C, 4 h	1.66	1.75	1.2	4.2
NBN30, 530 °C, 10 h	1.68	1.82	1.9	3.9

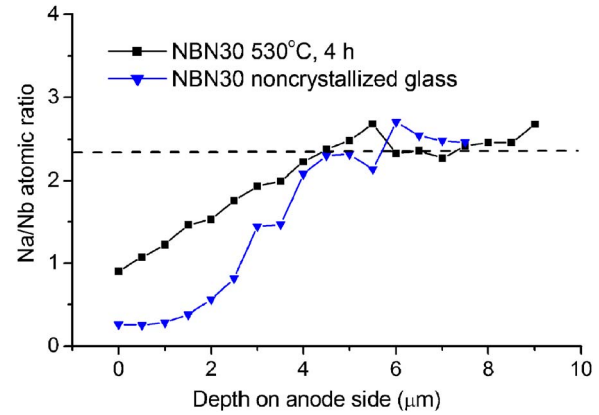


FIG. 5. (Color online) Cross section profile of the Na/Nb atomic ratio at the anode zone of thermally poled samples: as-prepared NBN30 glass (triangles) and glass crystallized at 530 °C for 4 h (squares). The dashed line gives the theoretical Na/Nb atomic ratio in an NBN30 glass matrix.

phase: then, the glass matrix composition should be close to a pure borate glass. Finally, the thickness of the depleted layer ($\sim 4 \mu\text{m}$) is quite consistent with the SHG analysis (see Table I).

Consequently, results from the elemental analysis let us conclude that an internal electric field is created at the anode surface of both the glass and glass ceramic because of a strong sodium migration. This internal electric field induces then a second order optical nonlinearity both in the glass and the glass ceramic composites. Nevertheless, the origin of the enhancement of $\chi^{(2)}$ with crystallization is not straightforward. Two mechanisms may be invoked that give large values of second order optical nonlinearity in thermally poled crystallized glass.

The first mechanism could arise from the collective and coherent ferroelectric (or superparaelectric) response of the nanoparticles of NaNbO_3 dispersed in the glass matrix. Such a mechanism has been observed by Benino *et al.* in niobium germanate and tellurite glass ceramics containing small ferroelectric crystals.¹⁵ The authors have found that the SHG intensity detected in the bulk of composites increases with the applied external electric field $E \sim (0.5-2.0) \times 10^6 \text{ V/m}$. In our study, no SHG signal is observed in unpoled NBN30 crystallized glass. Therefore the crystallized particles of sodium niobate give no spontaneous polarization because either their structure is not ferroelectric or it is, but with an isotropic orientational averaging of the anisotropic ferroelectric nanocrystals. Our first observation is consistent with the fact that the pure NaNbO_3 phase is antiferroelectric at room temperature and atmospheric pressure.¹⁶ In addition, numerous phase transitions between different ferroelectric and antiferroelectric modifications of NaNbO_3 have been observed between room temperature and 460 °C, which is the last phase transition temperature that stabilizes a paraelectric cubic phase.¹⁷ Also, ferroelectric properties can be induced in sodium niobate crystals by doping them or when applying an external electric field. Konieczny has reported a ferroelectric response in a NaNbO_3 single crystal thermally poled at 200 °C under an electric field of $7 \times 10^5 \text{ V/m}$.¹⁸ The internal electric field created during thermal poling within the glass can be as large as 10^9 V/m in silica glasses¹ and 10^8 V/m in

sodium niobium borophosphate glasses.¹⁹ Such a strong electric field should be able to induce a polarization in crystallites of sodium niobate despite the small size of the particles that should also feel an internal mechanical stress. The size of particles is rather small to expect ferroelectric response of NaNbO_3 but superparaelectric effect may appear in small crystals. Considering the small size and assuming a homogeneous distribution of the crystal particles in the glass, one should expect the occurrence of a thin nonlinear optical layer at the anode surface of the composite after thermal poling.

The second mechanism, responsible for the SHG response of the plates after thermal poling, is connected to Eq. (1) (EFISHG process). The crystallization of sodium niobate can increase the average value of $\chi^{(3)}$ in the glass ceramic composite. Consequently, the second order optical nonlinearity in thermally poled glass containing small particles of sodium niobate should increase. Shioya *et al.* have reported modification of $\chi^{(3)}$ with crystallization of potassium niobium tellurite glasses.²⁰ More recently, Lipovskii *et al.* observed a significant increase of the nonlinear refractive index n_2 (related to $\chi^{(3)}$) measured at $\lambda=1064$ nm in silicate glasses where a crystallization of NaNbO_3 occurs.²¹ An enhancement of the nonlinear refractive index n_2 from $+0.2 \times 10^{-14}$ to $+0.5 \times 10^{-14}$ cm²/W has been observed in composites with small crystal size of NaNbO_3 particles (~ 10 nm). The values of the Kerr coefficients could be correlated to the concentration of crystal particles, in good agreement with the Maxwell-Garnet model.²² A similar behavior may be expected in NBN30 glass ceramic since a crystallization of the sodium niobate phase takes place.

At the present time, for the poled glass ceramic composites under study, we are not able to exclude one of these two mechanisms. It is difficult to separate the contributions of these mechanisms since they both depend on the value of the internal electric field. The symmetry of both effects should be similar. Further investigations, including evaluation of quantity and size of NaNbO_3 particles by electron microscopy, measurements of $\chi^{(3)}$, and studies of the dielectric properties, are in progress.

IV. CONCLUSION

Glass ceramic composites were prepared by bulk crystallization of NaNbO_3 in sodium niobium borate glasses. Thermal poling of as-prepared glasses and glass ceramic samples induces a SHG signal in all samples. A sodium depleted region at the anode side, detected by EDX measurements, is evidence of an internal electric field induced at the anode surface of the poled samples. The second order NLO response of poled NBN30 glass ($\chi^{(2)} \sim 0.2$ pm/V) is much weaker than that of sodium niobium borophosphate glass ($\chi^{(2)} \sim 5$ pm/V). The NLO response $\chi^{(2)}$ of poled glass ce-

ramic composites increases with the rate of crystallization of sodium niobate that also increases the size of the crystallized particles. It reaches a value of 1.9 pm/V in a sample crystallized during 10 h at 530 °C. Two mechanisms may be considered to explain this phenomenon: first, a spontaneous ferroelectric response arises from NaNbO_3 nanocrystallites (pure structural $\chi^{(2)}$ process) and second, the internal electric field increases the $\chi^{(3)}$ response of the nanocrystallites and an EFISHG process occurs. Further investigations are necessary to detail the nature of the large second order nonlinearity observed in NBN30 glass ceramic.

ACKNOWLEDGMENTS

The authors acknowledge the program ANR-REGLIS "Research and Education in Glass and Laser Interaction Science" for financial support. One of the authors (A.M.) is grateful to the French government for the scholarship. Another author (V.R.) is indebted to the Région Aquitaine and the University of Bordeaux Sciences and Technologies for financial support in optical, laser, and computer equipment.

¹R. A. Myers, N. Mukherjee, and S. R. J. Brueck, *Opt. Lett.* **16**, 1732 (1991).

²N. Mukherjee, R. A. Myers, and S. R. J. Brueck, *J. Opt. Soc. Am. B* **11**, 665 (1994).

³P. G. Kazansky and S. St. J. Russel, *Opt. Commun.* **110**, 611 (1994).

⁴GLAMOROUS project, <http://www.glamorous-eu.com>

⁵M. Dussauze, E. Fargin, M. Lahaye, V. Rodriguez, and F. Adamietz, *Opt. Express* **13**, 4064 (2005).

⁶M. Guignard, V. Nazabal, J. Troles, F. Smektala, H. Zeghlache, Y. Quiquempois, A. Kudlinski, and G. Martinelli, *Opt. Express* **13**, 789 (2005).

⁷V. G. Dmitriev, G. G. Gurzadyan, and D. N. Nikogosyan, *Handbook of Nonlinear Optical Crystals* (Springer, Berlin, 1991).

⁸H. Jain, *Ferroelectrics* **306**, 111 (2004).

⁹Y. Takahashi, Y. Benino, T. Fujiwara, and T. Komatsu, *Appl. Phys. Lett.* **81**, 223 (1999).

¹⁰M. M. Layton and J. W. Smith, *J. Am. Ceram. Soc.* **58**, 435 (1975).

¹¹N. S. Prasad, K. B. R. Varma, Y. Takahashi, Y. Benino, T. Fujiwara, and T. Komatsu, *J. Solid State Chem.* **173**, 209 (2003).

¹²N. Tamagawa, Y. Benino, T. Fujiwara, and T. Komatsu, *Opt. Commun.* **217**, 387 (2003).

¹³A. Narazaki, K. Tanaka, and K. Hirao, *Appl. Phys. Lett.* **75**, 3399 (1999).

¹⁴V. Rodriguez and C. Sourisseau, *J. Opt. Soc. Am. B* **19**, 2650 (2002).

¹⁵Y. Benino, Y. Takahashi, T. Fujiwara, and T. Komatsu, *J. Non-Cryst. Solids* **345**, 422 (2004).

¹⁶G. Shirane, R. Newnham, and R. Pepinsky, *Phys. Rev.* **96**, 581 (1954).

¹⁷H. D. Megaw, *Ferroelectrics* **7**, 87 (1974).

¹⁸K. Konieczny, *Mater. Sci. Eng., B* **60**, 124 (1999).

¹⁹M. Dussauze, E. Fargin, A. Malakho, V. Rodriguez, T. Buffeteau, and F. Adamietz, *Opt. Mater. (Amsterdam, Neth.)* **28**, 1417 (2006).

²⁰K. Shioya, T. Komatsu, H. G. Kim, R. Sato, and K. Matusita, *J. Non-Cryst. Solids* **189**, 16 (1995).

²¹A. A. Lipovskii, D. K. Tagantsev, B. V. Tatarintsev, and A. A. Vetrov, *J. Non-Cryst. Solids* **318**, 268 (2003).

²²E. L. Falcao-Filho, C. A. C. Bosco, G. S. Maciel, L. H. Acioli, C. B. de Araujo, A. A. Lipovskii, and D. K. Tagantsev, *Phys. Rev. B* **69**, 134204 (2004).

²³JCPDS Card No. 74-2462, S. P. Solov'ev, Y. N. Venevtsev, and G. S. Zhdanov, *Kristallografiya* **6**, 218 (1961).